INTRINSIC AND FORCED INTERANNUAL VARIABILITY OF THE GULF OF ALASKA MESOSCALE CIRCULATION

A Thesis
Presented to
The Academic Faculty

By

Vincent Combes

In Partial Fulfillment
Of the Requirements for the Degree
Master of Science in the
School of Earth and Atmospheric Sciences.

School of Earth and Atmospheric Sciences
Georgia Institute of Technology
May 2007

INTRINSIC AND FORCED INTERANNUAL VARIABILITY OF THE GULF OF ALASKA MESOSCALE CIRCULATION

Approved by:

Dr. Emanuele Di Lorenzo, Advisor
School of Earth and Atmospheric Sciences
Georgia Institute of Technology

Dr. Robert Dickinson
School of Earth and Atmospheric Sciences
Georgia Institute of Technology

Dr. Rong Fu
School of Earth and Atmospheric Sciences
Georgia Institute of Technology

Date Approved: April 2, 2007

TABLE OF CONTENTS

LIST OF TABLES

LIST OF FIGURES

SUMMARY

The response of the Gulf of Alaska (GOA) circulation to large-scale North Pacific climate variability is explored using three high resolution (15 km) regional ocean model ensembles over the period 1950-2004. On interannual and decadal timescales the mean circulation is strongly modulated by changes in the large scale climate forcing associated with PDO and ENSO. Intensification of the model gyre scale circulation occurs after the 1976-1977 climate shift, as well as during 1965-1970 and 1993-1995. From the model dynamical budgets we find that when the GOA experiences stronger southeasterly winds, typical during the positive phase of the PDO and ENSO, there is net large-scale Ekman convergence in the central and eastern coastal boundary. The geostrophic adjustment to higher sea surface height (SSH) and lower isopycnals lead to stronger cyclonic gyre scale circulation. The opposite situation occurs during stronger northwesterly winds (negative phase of the PDO).

Along the eastern basin, interannual changes in the surface winds also modulate the seasonal development of high amplitude anticyclonic eddies (e.g. Haïda and Sitka eddies). Large interannual eddy events during winter-spring, are phase-locked with the seasonal cycle. The initial eddy dynamics are consistent with a quasi-linear Rossby wave response to positive SSH anomalies forced by stronger downwelling favorable winds (e.g. southwesterly during El Niño). However, because of the fast growth rate of baroclinic instability and the geographical focusing associated with the coastal geometry,

most of the perturbation energy in the Rossby wave is locally trapped until converted into large scale nonlinear coherent eddies. Coastally trapped waves of tropical origin may also contribute to positive SSH anomalies that lead to higher amplitude eddies. However, their presence does not appear essential. The model ensembles, which do not include the effects of equatorial coastally trapped waves, capture the large Haïda and Sitka eddy events observed during 1982 and 1997 and explain most of the variance of tidal gauges along the GOA coast.

In the western basin, interannual eddy variability located south of the Alaskan Stream is not correlated with large scale forcing and appears to be intrinsic. A comparison of the three model ensembles forced by NCEP winds and a multi-century-long integration forced only with the seasonal cycle, shows that the internal variability alone explains most of the eddy variance. The asymmetry between the eddy forced regime in the eastern basin, and the intrinsic regime in the western basin, has important implications for predicting the GOA response to climate change. Eastern boundary eddies transport important biogeochemical quantities such as iron, oxygen and chlorophyll-a into the gyre interior, therefore having potential upscale effects on the GOA high-nutrient-low-chlorophyll region.

CHAPTER I

INTRODUCTION

The Gulf of Alaska (GOA) is a semi-enclosed basin strongly controlled to atmospheric changes. Observational and modeling studies suggest that decadal-scale variability in the gyre circulation is consistent with an oceanic response to wind forcing (Lagerloef 1995; Cummins and Lagerloef, 2004). Interannual variability in wind stress over the GOA is correlated with the Pacific Decadal Oscillation (PDO) and the Southern Oscillation. Intensification of the Aleutian low during 1976-77, also referred to as the "climate shift" (Miller et al., 1994) modified the surface ocean circulation of the GOA (Capotondi et al., 2005; Miller et al., 2005). More specifically, Miller et al. (2005) suggest that an intensification of the Alaskan Stream occurred after the 1976-1977 climate shift, although the Alaska Current and eddies generated on the eastern GOA remain mostly unchanged. In addition to local changes in surface winds, coastally trapped Kelvin waves generated in the tropics during the El Niño Southern Oscillation (ENSO) affect the GOA circulation (Meyers and Basu, 1999).

Despite the numerous observational studies over the northeast Pacific Ocean (Brickley and Thomas, 2004; Crawford, 2002; Ladd et al, 2005; Meyers and Basu, 1999; Strub and James, 2002), important aspects of the GOA dynamics (e.g., mesoscale activity) have been rarely studied or modeled, and thus are not well understood. Some

modelers have nevertheless focused their studies on mesoscale circulation in the GOA, such as Haïda or Sitka eddies (Melsom et al, 1999; Di Lorenzo et al., 2005a). Okkonen et al. (2001) have also suggested that eddy variability is dominated by the local response to wind forcing along the Alaska Current (eastern GOA basin) and is non-deterministic in the Alaskan Stream (western GOA basin).

Eddies in the GOA have already been studied for several decades using available observations (Tabata, 1982). In the eastern GOA basin, three major groups of eddies have been identified according to the location of their formation, Yakutat, Sitka and Haïda (Fig. 1). These three eddy groups share common features, such as an anti-cyclonic rotation (up to 0.4m sea surface height anomaly) with a warmer and less saline core above 100m depth. (Tabata, 1982; Crawford, 2002). The generation and migration of these eddies, which can survive for more than three years, is well documented in satellite observations (Thomson and Grower, 1998; Crawford, 2002). Haïda and Sitka eddies mostly propagate offshore while the Yakutat eddies propagate alongshore along the western basin. While previous studies attribute the generation of these large eddies to baroclinic instability of the coastal currents (Thomson and Grower, 1998; Murray et al. 2001), a more recent numerical investigation by Di Lorenzo et al. (2005a) suggests that the most southern eddy, the Haïda eddy, can develop without instabilities by simple advection of buoyant water masses around Cape St. James (southern tip of Queen Charlotte Island). These advected water masses generate patches of buoyant flow with anticyclonic circulation which merge to generate larger eddies when the flow around the cape is strong. For the more northern Sitka and Yakutat eddies a more detailed modeling study of their formation has not been completed.

In addition to the eddies developed in the eastern boundary, the western basin also exhibits enhanced eddy activity. Along the Alaskan Stream, eddies have been both observed (Crawford et al., 2000) and modeled (Okkonen et al., 2001) and tend to propagate southwestward along the Aleutian peninsula. In the Shelikof sea valley (north GOA basin) Stabeno and Hermann (1996) find a good agreement between eddies generated by a model and observations, however their study does not diagnose the eddy dynamics.

Understanding the dynamics of eddies and other mesoscale physical processes is critical for predicting how tracer exchanges between inshore and offshore water masses will respond to changes in atmospheric and ocean state (e.g. ENSO, PDO, global climate change). For example eddies have several direct implications on the climate and biology of the GOA, because of their important role in cross-shelf transport. A recent study suggest that about 35% to 60% of northward heat transport during winter is carried offshore by the eastern basin large eddies (Crawford, 2005). Crawford (2005) estimates that 15% of the total river freshwater input between the Columbian River and 54N is transported by these eddies. Nutrient exchanges (Ladd et al, 2005; Whitney and Robert, 2002) and iron transport (Johnson et al., 2005) also occur vertically in the core of eddies. The eddy induced transport is also linked to the biological productivity in the offshore high nutrient low CHL-a (HNLC) waters of the Alaskan gyre (Crawford et al. 2007). Links between eddy transport, water mass properties and biota have also been reported in the GOA western basin (Okkonen et al., 2003). At the higher trophic levels the link between mesoscale processes and species distributions/abundance has not been fully established. However fish communities have been found to respond strongly to large-

scale atmospheric changes, such as the 1976-77 climate shift (Litzow et al., 2006; Mantua et al., 1997). Potentially some of these changes may be related to changes in eddy transport statistics as hypothesized by Miller et al. (2005) in a study of the Steller sea lions decline in the western GOA. Other important mechanisms for cross-shelf fluxes in the GOA include episodic upwelling, surface flux in the Ekman layer, upwelling seaward of a coastal wind jet and topographic steering (Stabeno et al., 2004).

In order to further clarify the mean, seasonal and interannual response of the GOA mesoscale circulation to atmospheric changes, we conduct numerical investigations with a high-resolution ocean model. Three ensembles, forced by the last 55 years of NCEP/NCAR wind stress reanalysis (Kalnay et al., 1996) and heat fluxes corrected using the NOAA extended SST (Smith and Reynolds, 2004), are used to separate the intrinsic and forced variability in the GOA. The primary goals of this study are to (1) understand how the surface circulation and eddy statistics are controlled by atmospheric forcing at the seasonal and interannual timescale, and (2) separate the intrinsic and forced variability in the GOA.

This paper is organized as follows. Section 2 describes the model experiments and the domain used for this study. Section 3 discusses the mean circulation in the GOA and its interannual modulations by changes in surface forcing during different phases of the PDO. Section 4 looks at the seasonal and eddy circulation in the western and eastern basin. A summary is provided in section 5.

CHAPTER II

MODELING APPROACH AND DOMAIN

The Regional Ocean Modeling System (ROMS, Haidvogel et al., 2000, Shchepetkin and McWilliams, 2005) is used to investigate the forced and intrinsic variability of the Gulf of Alaska circulation. ROMS is a free-surface, hydrostatic, eddy-resolving primitive equation ocean model that uses stretched, terrain-following coordinates in the vertical and orthogonal curvilinear coordinates in the horizontal. The hydrostatic primitive equations are solved using a split-explicit time-stepping scheme, which allows the separation of the barotropic and baroclinic components of the momentum equations with internal and external time steps. Different resolutions and different domains have previously been used with the ROMS model and provide reliable results for the North Pacific Ocean (Marchesiello et al., 2003, Di Lorenzo et al. 2005b, Curchister et al., 2005, Miller at al., 2005).

The grid extends northward from 25N to 61N and westward from -111W to -179W. The average spatial resolution is between 19km (South) to 13.4 km (North) with 30 vertical levels (with higher resolution at the upper ocean layer), that is to say a total number of 1,697,280 points (Latitude x Longitude x Depth = 272 x 208 x 30). The domain of interest for this study includes all of the Gulf of Alaska from Washington State to the northern boundary. In order to avoid large pressure gradient errors (Mellor et al,

Table 1: Table of experiments

	Run length	Initial conditions	Open boundaries	Surface Forcing
Experiment 1	163 years (53+55+55)	Levitus et al. (1994)	Temperature, Salinity and Geostrophic Velocity derived from Levitus et al. + nudging	55 years wind stress of NCEP/NCAR heat fluxes corrected with NOAA extended SST fresh water fluxes from corrected climatology
Experiment 2	163 years (53+55+55)			monthly climatological forcings derived from Experiment 1 forcing functions.

1994), the model bathymetry is obtained by a smooth interpolation from David T. Sandwell and Walter H. F. Smith bathymetry. This complete bathymetric map of the oceans has a 3-10 km resolution by combining all the information provided by the Geosat, ERS-1/2, Topex/Poseidon altimeters, and available depth soundings (Sandwell and Smith, 1997, Smith and Sandwell, 1994).

Experiment 1 (Table 1) consists of 3 ensembles, each forced by the last 55 years of NCEP/NCAR (National Center for Environmental Prediction/National Center for Atmospheric Research) wind stress reanalysis (Kalnay et al., 1996) and by heat fluxes corrected using the NOAA (National Oceanic & Atmospheric Administration) extended SST (Smith and Reynolds, 2004). The freshwater surface fluxes are set to a corrected monthly climatology derived during an 80 year long spinup run in which the surface salinity is nudged to the observed climatology and the resulting flux correction is saved.

Experiment 2 differs from Experiment 1 in the surface forcing conditions, which are prescribed to the monthly mean climatology. The initial and boundary conditions remain unchanged. We refer to Experiment 2 as the “Unforced Run”, in that there is no forcing function with periodicity longer than the seasonal cycle. In contrast, Experiment 1, which

is forced by the time dependent NCEP winds and NOAA SST, is referred to as the "Forced Run".

For the initial condition, zonal and meridional velocity, sea surface height, temperature, and salinity are obtained from Levitus data (1994). At the open boundaries the model uses a modified radiation condition (Marchesiello et al., 2001) together with nudging to prescribed monthly climatologies for temperature, salinity and geostrophic velocity derived from Levitus et al. (1994). The geostrophic velocity is computed using a reference level of 1000 m.

CHAPTER III

MEAN AND INTERANNUAL CIRCULATION

The circulation in the GOA is mainly described by the subarctic gyre (Figure 1). On the eastern boundary of the GOA basin, the North Pacific Drift diverges into the southward California Current and the northward Alaska Current. The Alaska Current is rich in meanders and eddies, such as Haïda and Sitka along the eastern boundary. As the Alaska Current flows along the Alaska Peninsula it becomes the Alaskan Stream, which has a more developed and richer eddy field associated with the strong instability of the mean currents. Near the Kodiak Island, the Alaskan Stream is narrow (about 50 km) and strong (50 cm s^{-1}) (Stabeno et al, 2004). The currents are principally in geostrophic balance and consequently follow lines of constant dynamic height with the largest values on the right. The model mean circulation, represented in Figure 1b by the sea surface height (SSH), is mostly consistent with this view described in the literature. In the eastern basin we find a broad northward current, corresponding to the Alaska Current, and an intensification of surface currents along the Aleutian Islands in the location of the Alaskan Stream. A map of the SSH standard deviation (Figure 1c) shows high variance in regions of intense eddy variability along the southern edge of the Alaskan Stream, along the eastern basin, and in the coastal regions where the variability is directly forced by changes in the atmospheric winds (a discussion follows in section 4). On the eastern

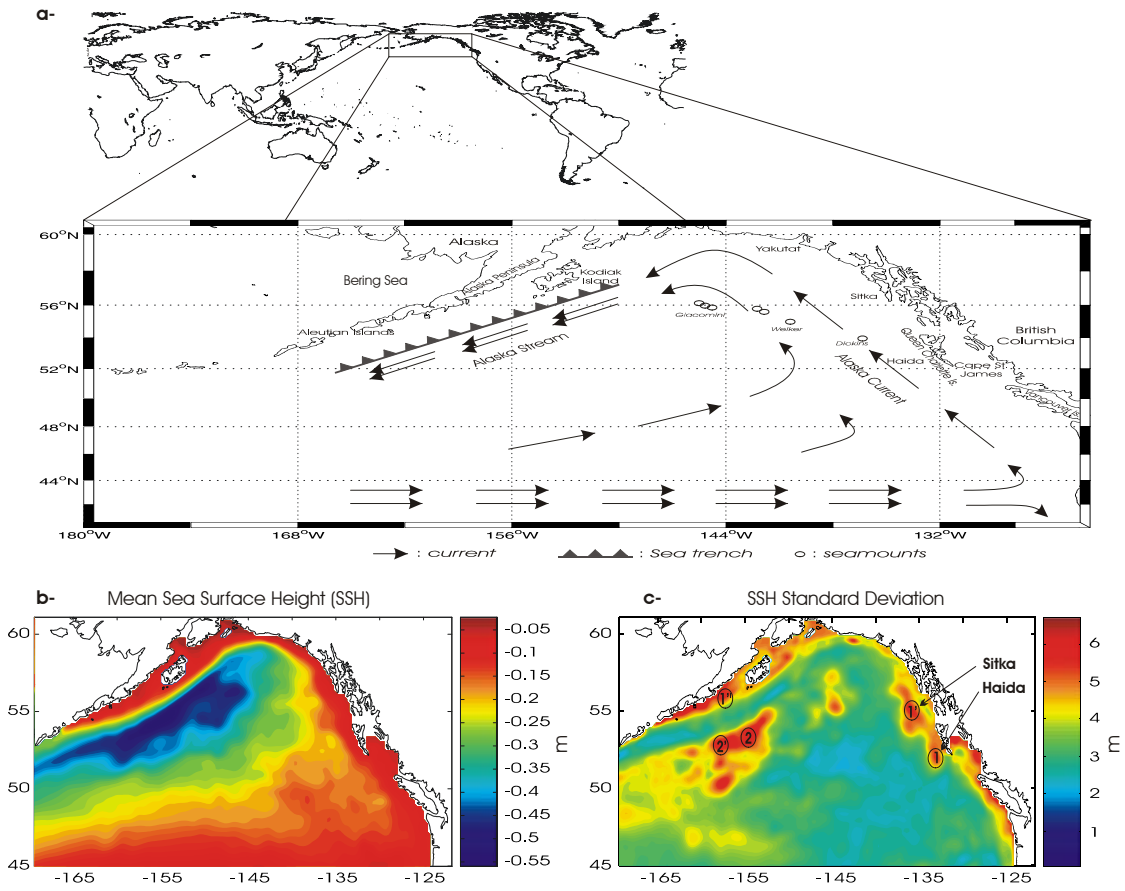

Figure 1: (a) Map of the domain (Gulf of Alaska: GOA). (b) Mean and (c) standard deviation of the sea surface height (SSH)

boundary, maxima of standard deviation are found in the generation sites of the Haïda and Sitka eddies. A corresponding region of high variance is not found at the location of the Yakutat eddy, which is not well represented in the model.

A closer inspection of the model mean momentum budget for the surface layer confirms (Figure 2a) that the dominant balance is geostrophic, with a stronger Alaskan stream (0.4 m s^{-1}) following the topographic slope in the northwestern basin and a weak northward flow in the eastern basin. The model geostrophic flow along the coast results from the ocean adjustment to the mean downwelling conditions in the eastern basin and upwelling along the topographic slope in the western basin. This is inferred from the

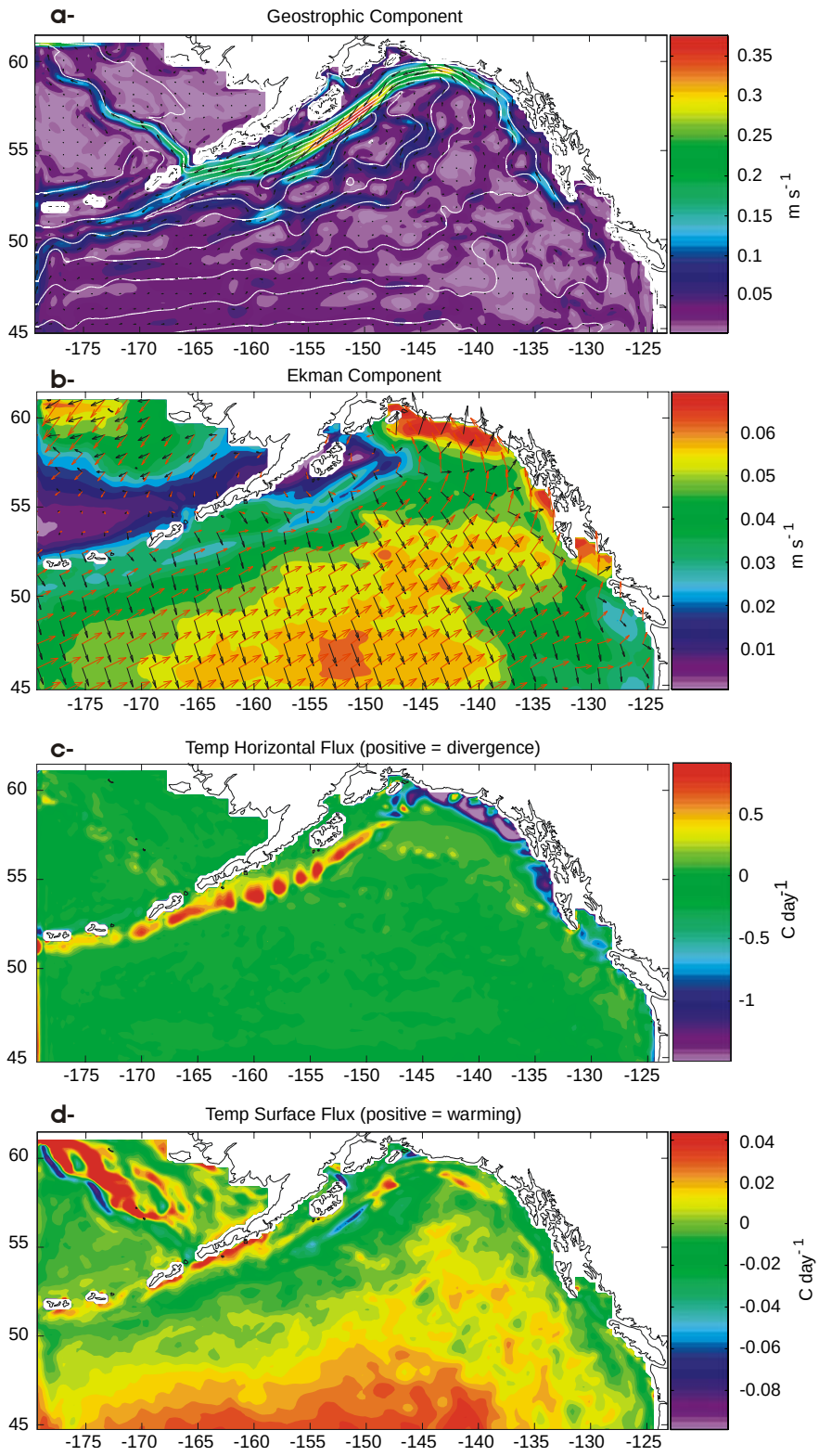

Figure 2: (a) Mean Geostrophic surface currents, with mean SSH contours (white lines). (b) Mean Ekman transport in model surface layer. The red arrow indicate the direction and intensity of mean surface wind stresses. (c) Temperature horizontal flux, positive regions indicate upwelling. (d) Temperature surface flux, positive indicate that the ocean is warming due to the atmospheric heat flux.

model Ekman currents averaged over the surface layer (Figure 2b) and the corresponding vertical fluxes of temperature (Figure 2c), which show regions of surface divergence in the west and convergence in the east. A detailed analysis of the temperature budget shows that the dominant balance is between the vertical and the horizontal flux. The next largest term in the budget, although still small compared to the advection terms, is the surface heat flux (Figure 2d). On average the surface heat fluxes are warming the Gulf of Alaska except in regions of strong downwelling (see blue areas in Figure 2c and 2d) where the strong horizontal convergence of surface warmer water tends to heat the atmospheric marine boundary layer and cool the ocean surface.

To investigate the interannual modulation of the mean circulation we compute the first Empirical Orthogonal Function (EOF) of the model SSHa, where the anomalies are defined by removing the seasonal cycle. The resulting EOF 1 (Figure 3a) explains 30% of the variance and has the same structure as the mean circulation. Temporal modulations in the amplitude and sign of this pattern are inferred from the Principal Component 1 (PC 1; Figure 3e) of the three ensemble members, and correspond to interannual and decadal changes in the mean circulation. The spread of the PCs 1 of the ensemble members is very small suggesting that changes in the mean circulation are mainly forced. Indeed strong interannual modulations of the PCs 1 correspond to changes in the monthly PDO index with a significant correlation of 0.64 (Figure 3f). Intensification of the gyre scale circulation is evident after the 1976-1977 climate shift, as well as during 1955-1960, 1965-1970 and more gradually during 1990-1998. Weakening of the circulations is evident during 1970-1975 and 1986-1991.

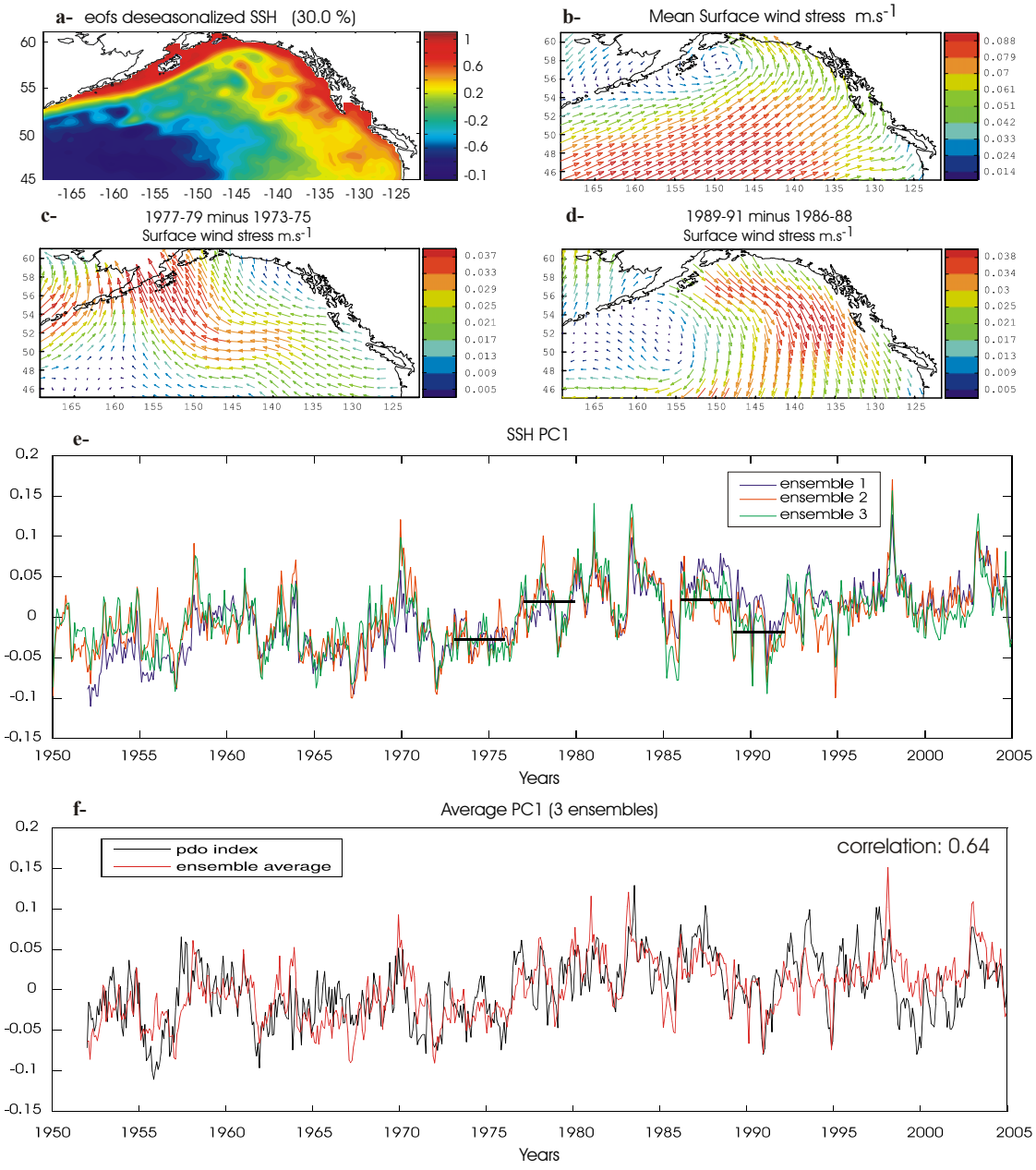

Figure 3: (a) First Empirical Orthogonal Function (EOF 1) of the sea surface height after removing the seasonal cycle. EOF1 explains 30.0% of the total variance. (b) Mean surface NCEP wind stress. (c) and (d) show the difference in surface wind stress for selected periods. (e) PC 1 for the three forced model ensembles. (f) Comparison between PDO index and PC1 ensemble average

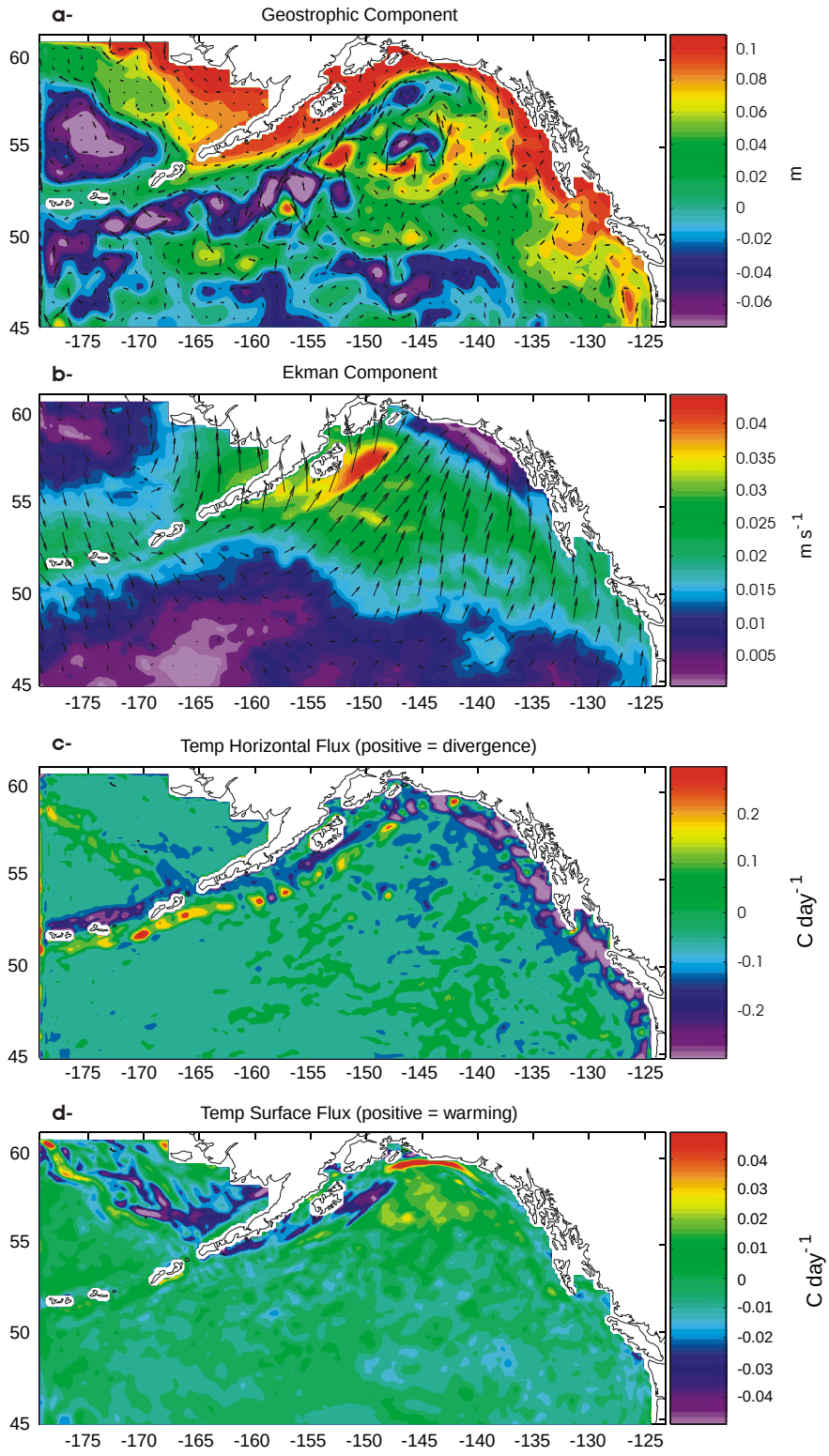

Figure 4: Difference map for the periods (1977-80) minus (1970-1975). (a) Difference in SSH and Geostrophic surface currents (b) Difference Ekman transport in model surface layer. (c) Difference temperature horizontal flux, negative regions indicate stronger downwelling conditions after 1976. (d) Difference in temperature surface flux, positive indicate that the ocean is warming due to the atmospheric heat flux.

Composite maps of the difference in surface winds (Figure 3c and d) suggest that the gyre intensifies during anomalous southeasterly winds (stronger Aleutian low) and weakens when the winds are predominantly anomalous northwesterly. A detailed analysis of the model momentum and tracer budgets reveals that these extrema in the mean circulation are indeed forced by changes in the surface wind stresses (Figure 4 illustrates an example for the 1976 shift). In particular we find a strengthening of the gyre when the Ekman transport tends to converge mass towards the coastal boundary in the central Gulf of Alaska (Figure 4b). This condition is also associated with stronger that usual downwelling along the eastern boundary (Figure 4c) and upwelling along the Alaskan Stream. The contribution of surface heat fluxes are modest compared to the mechanical forcing.

The adjustment process of the gyre scale circulation in response to the interannual and decadal changes of the PDO and ENSO can be summarized as follows. When the GOA experiences stronger anomalous southeasterly winds (positive phase of the PDO as well as ENSO) there is net convergence of surface mass (downwelling conditions) in the central and eastern coastal boundary induced by Ekman transport (Figure 4b). This generates higher coastal SSHa (Figure 4a) and lowers the coastal isopycnals. The resulting geostrophically adjusted currents (Figure 4a) intensify the gyre scale circulation. The opposite situation occurs during stronger anomalous northwesterly winds (negative phase of the PDO). In the next section we continue to explore the ocean adjustment process to changes in the forcing by investigating how the changes in the winds are reflected in the eddy scale circulation.

CHAPTER IV

THE SEASONAL AND INTERANNUAL EDDY FIELD

To gain confidence in the degree of realism of the model simulation, we compare the model sea surface height seasonal anomalies to the one derived from the AVISO satellite maps (Figure 5). These maps (http://www.jason.oceanobs.com) merge data from T/P or JASON-1 + ERS-1/2 and Envisat satellites to produce sea level anomalies at weekly resolution from October 1992 to January 2005 on a 1/3ºx 1/3º Mercator grid. An annual oscillation of the SSHa along the coast is evident in both the model and satellite data. Consistent with Strub and James (2002) observational results, the sea surface height anomaly along the coast is positive during the winter months and negative in summer, leading to a strong SSHa gradient (stronger downwelling current) in winter and weak SSH gradient (weak current) in summer. From the analysis of the model budget terms, we find that this oscillation is driven from the seasonality in the wind stress and consequent Ekman currents. Following the strong downwelling conditions along the coast in the eastern basin, a clear westward propagation of the SSHa is evident in both model and satellite during March through July. As the positive SSHa detaches from the coast a rich eddy field develops off the shelf. Anticyclonic eddies become a prominent feature, particularly in the model where the signature of the seasonal development of the Haïda

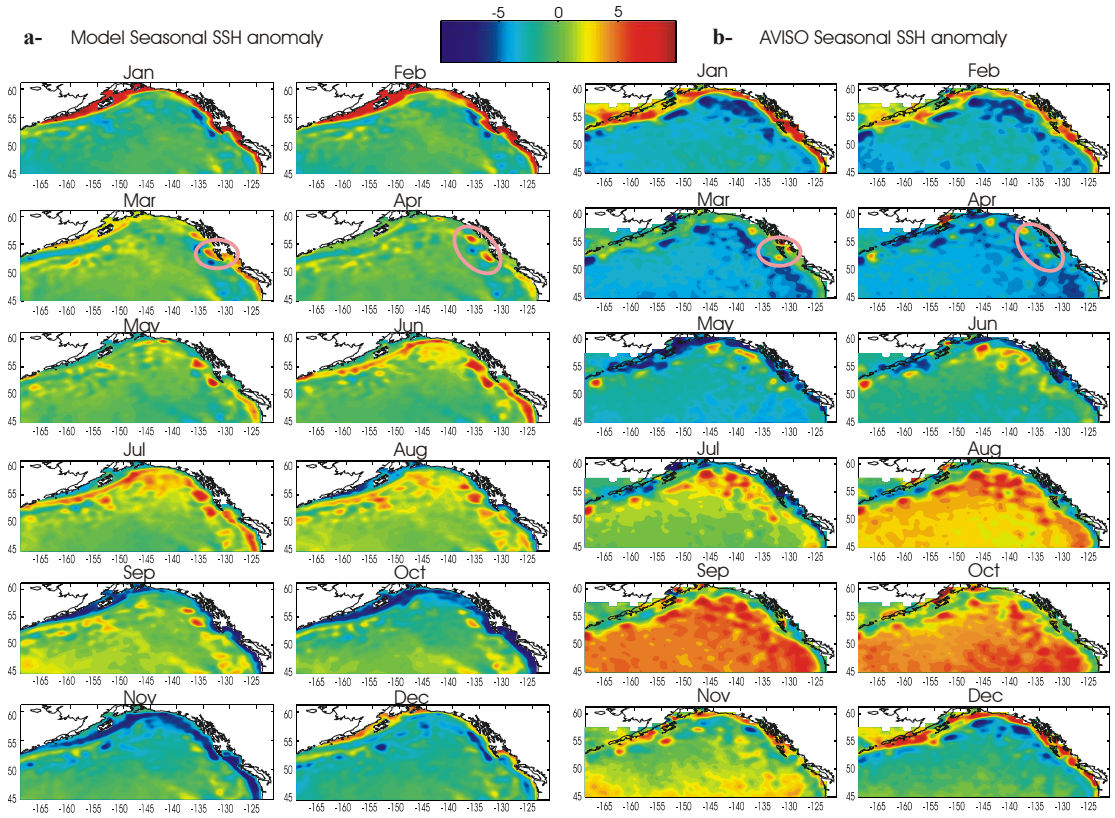

Figure 5: Model (a) and TOPEX (b) SSH seasonal anomalies derived from 1993 to 2004

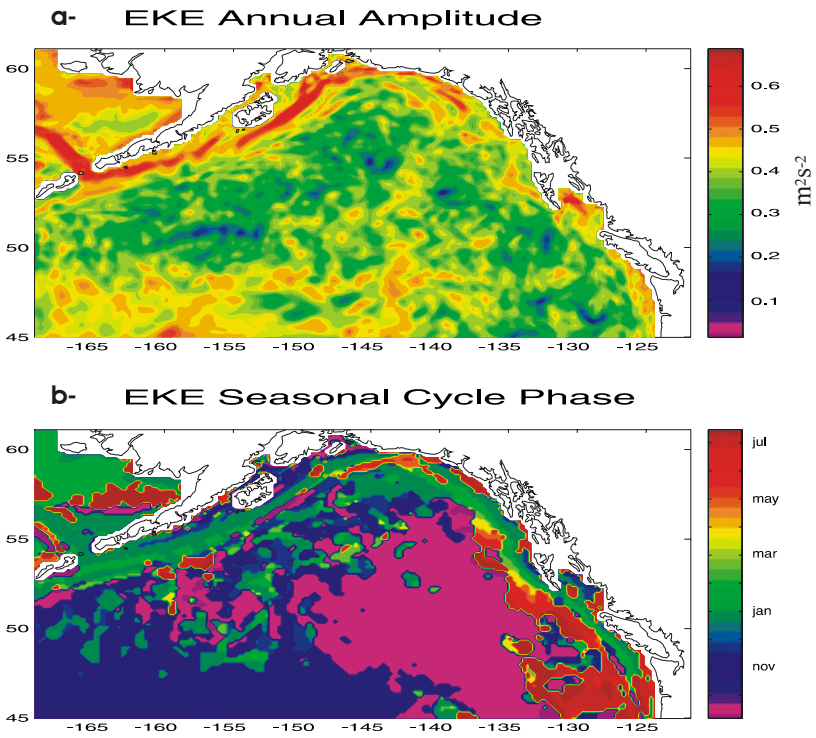

Figure 6: (a) Annual Amplitude of the Eddy Kinetic Energy (EKE) and (b) EKE Seasonal cycle phase

and Sitka eddies is quite strong when compared to satellite observations. In the western basin we also find a stronger mesoscale signature in July and August. Although both model and AVISO seasonal SSHa maps use the same time range, from January 1993 to December 2004, the satellite maps reveals an overall higher SSH anomalies in the gyre interior between August and October and lower between January and May. This difference in the seasonal amplitude variation of the gyre between model and observation may be explained by thermal expansion effects associated with biased heat flux forcing in the model simulation.

The seasonal development of the eddy field is also reflected in the eddy kinetic energy (EKE) phase map (Figure 6). Along the coast the seasonal maxima is reached in January when the stronger current develop on the shelf in response to the stronger downwelling conditions. During late spring/summer the EKE peak is found further away from the coast in the eastern basin and reflects the seasonal development of the eddy field. During the fall the seasonal peak moves further offshore in the gyre interior. The amplitude of the seasonal EKE is strongest on the shelf where the currents are directly forced by the winds (Figure 6a).

4.1 FORCED REGIME IN THE EASTERN BASIN

To better isolate the development of the large anticyclone along the eastern boundary we perform an analysis of the model SSHa EOFs 1 and 2 along the east coast (Figure 7). Consistent with the seasonal maps, the EOFs shows a spatially coherent excitation of SSHa along the coast (EOF 1) followed by offshore propagation (EOF2).

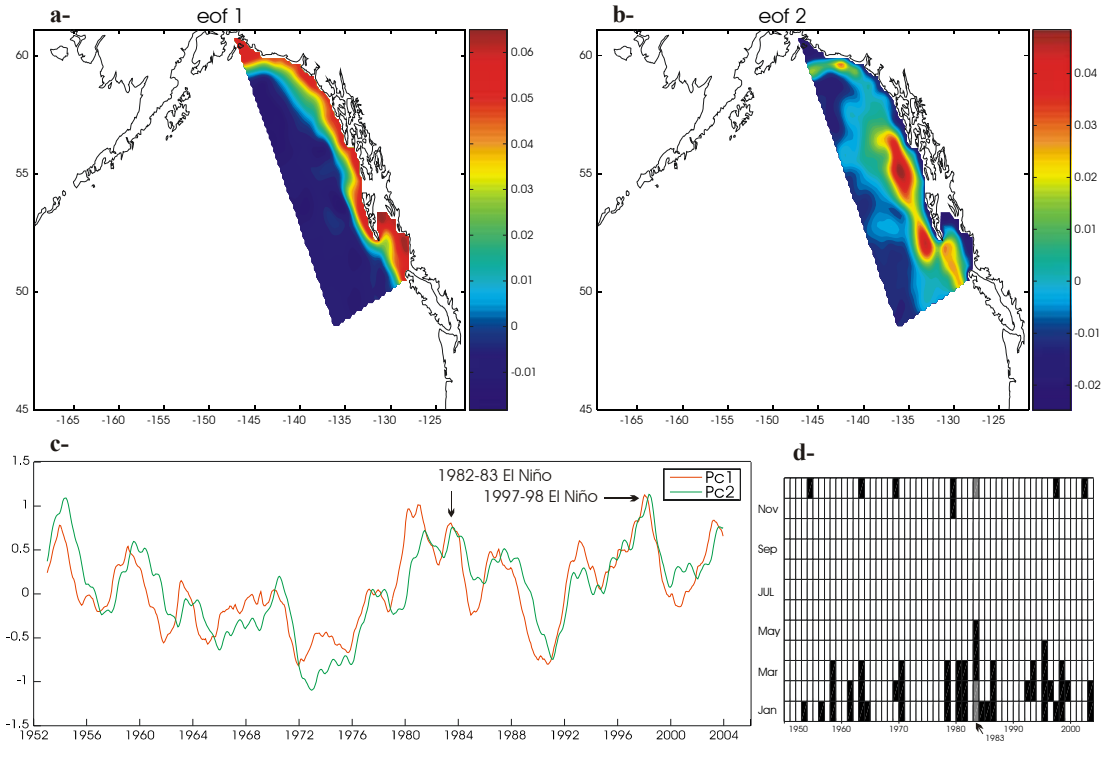

Figure 7: (a) EOF 1 and (b) EOF 2 of SSHa. (c) The red curve (green curve) is the principal component associated to EOF1 (EOF2), using a 1yr lowpass filter. (d) Matrix showing the times when large Haida eddies are formed in the model simulation

The major anticyclonic eddies in EOF 2, Haïda and Sitka, are captured by the model and exhibit substantial interannual variability as evident by the corresponding PCs (Figure 7c). Despite the two EOFs are uncorrelated, a 1 year low pass filter of PC1 and PC2 (Figure 7c) shows a 300 days lag, which confirms that the development of the two anticyclonic cores in EOF 2 (corresponding to Sitka and Haïda eddies) follow the SSHa of EOF 1. The two EOFs explained more than 54% of the variance. The same EOF analysis is performed for the specific region around the Queen Charlotte Islands, where Haïda eddies are generated (Figures not shown here). From this analysis we infer the speed of eddy propagation of 1.3 km day^{-1}, which is consistent with previous estimates of 1.12 ± 0.35 km day^{-1} by Gower and Tabata (1993). The PCs show that some of the largest events over the entire record correspond to strong El-Niño year, 1982-1983 and 1997-

1998. A table showing the year and month when large eddy events are found (Figure 7d) reveals that large Haïda and Sitka eddies are mainly generated during winter months (December, January, February, March) and are phase locked with the seasonal cycle. Therefore, interannual changes in the amplitude of the generated eddy are reflected in interannual modulation of the seasonal cycle.

To further clarify the relationship between the modeled eddies and El-Niño years, we perform the same EOF analysis for the three model ensembles and isolate the forcing patterns corresponding to large eddy events (Figure 8). We find that PCs 1 of all ensembles are correlated above 0.9 (Figure 8b and h) corroborating the hypothesis of a strongly forced regime. For the Haïda region, a composite analysis of the winter wind patterns during times when PC1 is greater than 1 and less than -1, shows that the winds are predominantly southwesterly (Figure 8c and d). However if we take the differences between the composites and the mean winds we find that during times of higher amplitude eddies (PC $1 \geq 1$) the winds are strongly downwelling (Figure 8e) and therefore capable of exciting stronger SSHa. In contrast during times of weaker amplitude eddies the winds have upwelling favorable anomalies (Figure 8f). The same analysis performed for the Sitka region leads to the same results (Figure 8g-l), mainly that stronger eddies are excited by stronger winter downwelling winds. An inspection of the composite map of the winter wind stress anomalies during the 1982 and 1997 El-Niños (Figure 9) confirm the existence of stronger downwelling winds, therefore explaining the observed correlation between El-Niño and large eddy events. In contrast the La-Niña events of 1970 and 1988 show upwelling favorable winds and reduced eddy amplitude.

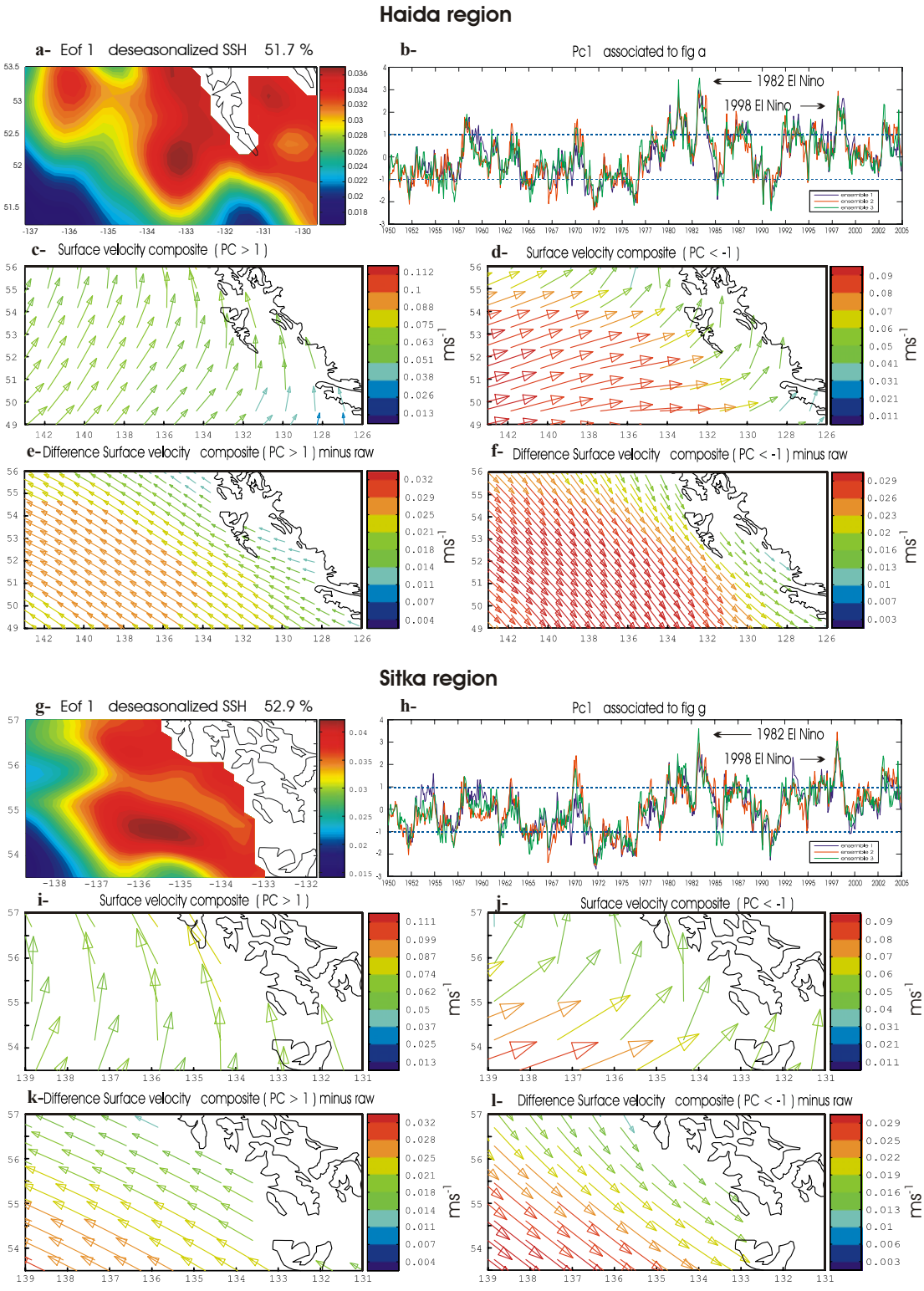

Figure 8: (a) EOF 1 and (b) PC 1 of SSHa in the region of formation of Haida eddies. (c)Wind stress composite maps for PC 1 > 1, (d) for PC 1 <- 1. (e)Wind stress anomaly composite maps for PC 1 > 1, (f) for PC 1 <- 1. (g-l) same as (a-f) but for Sitka region.

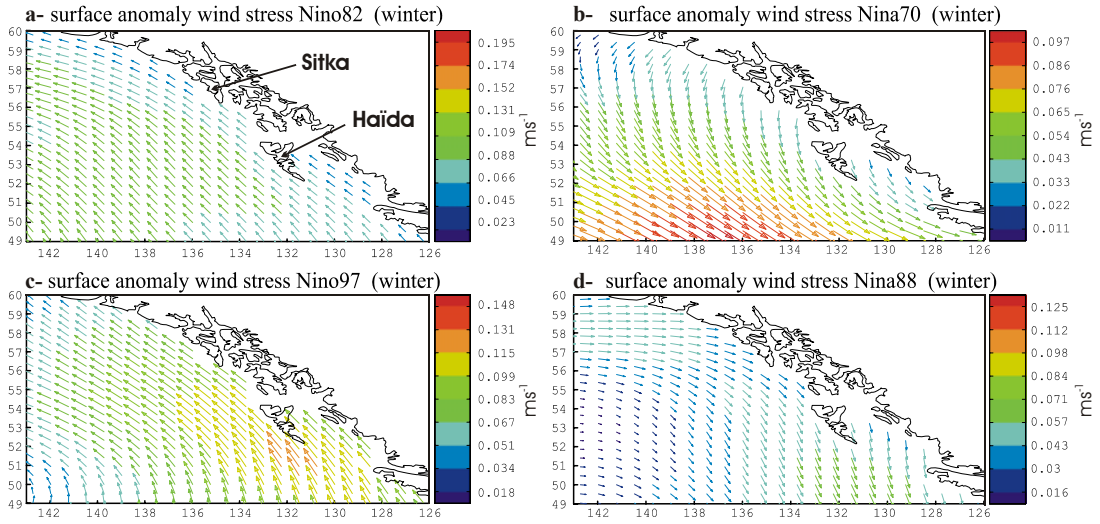

Figure 9: NCEP surface wind stress anomaly (with respect to the 1950-2004 period) for the El Niño winters (a) 1982-83, (c)1997-98 and (b) La Niña winters 1970-71, (d) 1988-89.

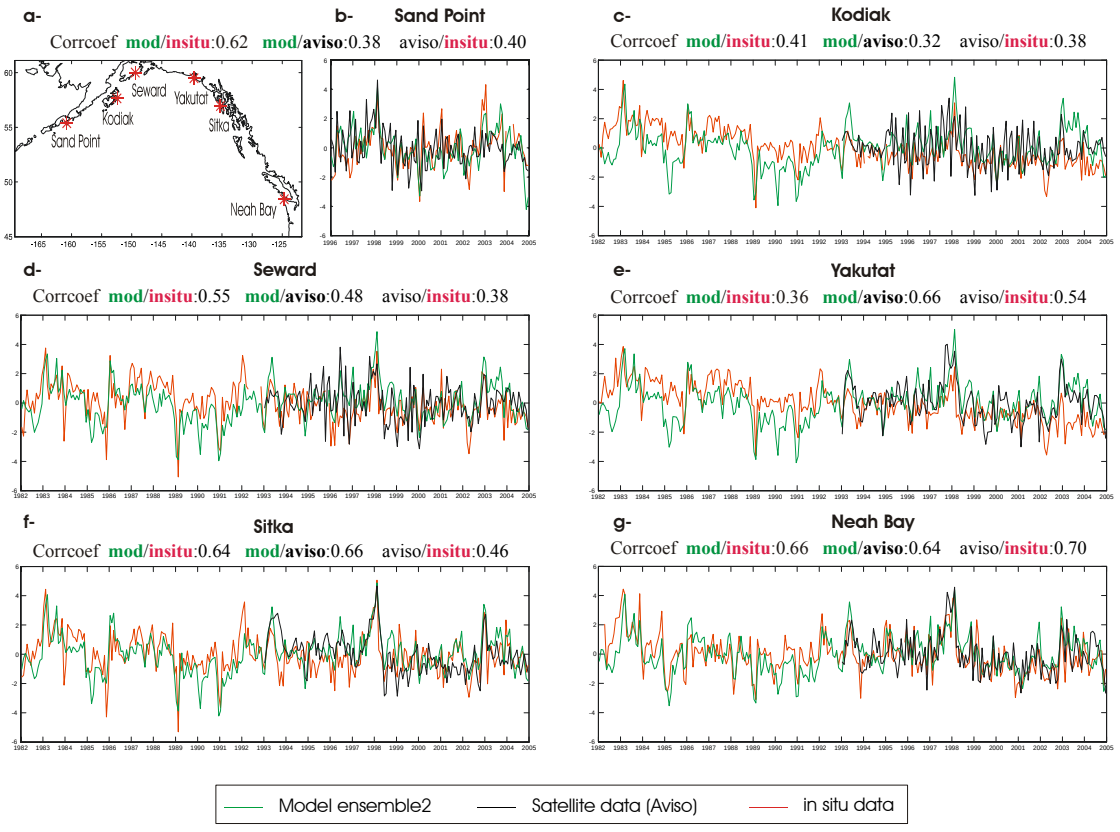

Figure 10: Comparison of the coastal deseasonalized SSH for Sand point, Kodiak, Seward, Yakutat, Sitka, and Neah Bay between the model output (green line), AVISO/TOPEX (black line) and GLOSS "fast delivery"data (red).

Excitation of positive SSHa along the coastal boundary can also be attributed to coastally trapped Kelvin waves of equatorial origin. Indeed Meyers and Basu (1999) indicate that Kelvin waves are a source of interannual variability in the coastal current along western North America. However, in this study we used a monthly mean climatology southern open boundary condition from Levitus et al. (1994), which does not include these tropically generated Kelvin-like waves. Nevertheless a comparison of the model coastal sea level with in situ records and satellite data in various coastal location (Sitka, Neah Bat, Seward, Yakutat, Kodiak and Sand Point; Figure 10) indicate that the model hindcast is able to explain a very large fraction of the SSH variance. For example at Sitka the model explains 41% of the in-situ observations variance, which is more than the satellite (21%). At other locations, except Yakutat, the model generally compares more favorably than the satellite with in situ data, implying that it captures a large fraction of the variance within the observational uncertainties. At Yakutat the correlation is not very high as the model does not reproduce Yakutat eddies very well. High correlations with in situ data are also found at coastal location along the Alaskan Stream. From these results we conclude that most of the interannual variability in the eastern boundary eddies and over the shelf, is locally forced by the winds, although coastally trapped waves may still contribute to additional variance.

We now discuss a dynamical framework to understand the relationship between the forcing and the development of large scale eddies in the eastern boundary. Previous studies suggest that the seasonal and interannual development of the mesoscale eddy field results from instability associated with the seasonal mean coastal currents and buoyancy gradients (Thomson and Grower, 1998; Melson et al., 1999; Okkonen et al., 2001;

Murray et al., 2001). Although other studies show alternative generating dynamics for these eddies (Di Lorenzo et al. 2005a) we reframe the current and previous findings in the context of instability of linear Rossby waves. This follows from the observation that EOF 1 and EOF 2 (Figure 7) are consistent with a linear excitation and propagation of a Rossby wave. LaCasce and Pedlosky (2004) show using an idealized setup, that Rossby waves excited at the eastern coastal boundary are subject to baroclinic instability, in particular when the growth rate of the instability is fast compared to the time it takes for the wave to cross the ocean basin. Because the phase speed of Rossby waves decreases with increasing latitude, first mode baroclinic Rossby wave phase speeds are extremely slow in the Gulf of Alaska (about 1-2 km/day from Chelton and Schlax (1996)). Indeed during winter, following the strong downwelling condition, the linear adjustment process to the positive sea level perturbations (seasonal in Figure 5a, interannual in Figure 7) leads to radiation of Rossby waves that would take about 6 months to propagate away from the excitation region, in this case the coastal boundary. This timescale agrees with the observed and modeled SSHa propagation away from the east coast during winter and spring (Figure 7). However, LaCasce and Pedlosky (2004) theory predicts that the excited Rossby waves become unstable at higher latitudes and will not have time to coherently propagate in the gyre interior. Both model and observations (Chelton and Schlax, 1996) support this view and do not show a meridionally coherent westward phase propagation.

To verify if the LaCasce and Pedlosky (2004) theory is applicable for the Gulf of Alaska, we compare the propagation timescale of the waves with the typical growth rate of baroclinic instability in the Gulf as inferred by the Eady index (Lindzen and Farell, 1980) defined:

$$\sigma_E = 0.31 \frac{f}{N} \frac{du}{dz}$$

where f is the Coriolis parameter (s^{-1}), $N^2 = -\frac{g}{\rho_0} \frac{d\rho}{dz}$ represents the static stability (s^{-2}) and ρ the density of water (kg m^{-3}). In the computation, we consider *u* as the current speed. The Eady index, σ_E, is then integrated between the surface and 100m meters depth. Although σ_E describes the baroclinic instability of a zonal basic-state flow (Hoskins and Valdes, 1990) it still provides a rough estimate of the typical growth rate of the instabilities and is similar to the criteria used by LaCasce and Pedlosky (2004) which use the ratio between vertical shear and Rossby deformation radius. Figure 11 shows the model monthly mean maps of the Eady index, which exhibit a clear seasonal cycle with higher baroclinicity during winter. Between October and April along the coast where the SSHa is perturbed by the seasonal peak of downwelling winds, the Eady index has values between 4 and 7 x 10^{-6} s^{-1}. The corresponding timescale for the growth rate of the instability is of 2-6 days, which is much too fast for the coastal disturbances to radiate away as Rossby waves.

The reoccurrence of large anticyclones at the same regional locations (e.g. Haïda, Sitka and Yakutat) has been reported in several observational (Crawford, 2002) and modeling studies, some of which suggest the possibility for mechanisms other than instabilities to be equally important in the generation of the eddies (Di Lorenzo et al. 2005a). The LaCasce and Pedlosky (2004) theory does not explicitly account for the geographical location of the major anticyclonic eddies. However it is likely that during the linear phase of the ocean adjustment process to the wind induced isopycnal perturbations (EOF 1 and 2 Figure 7), the SSHa amplitude is heavily influenced by the

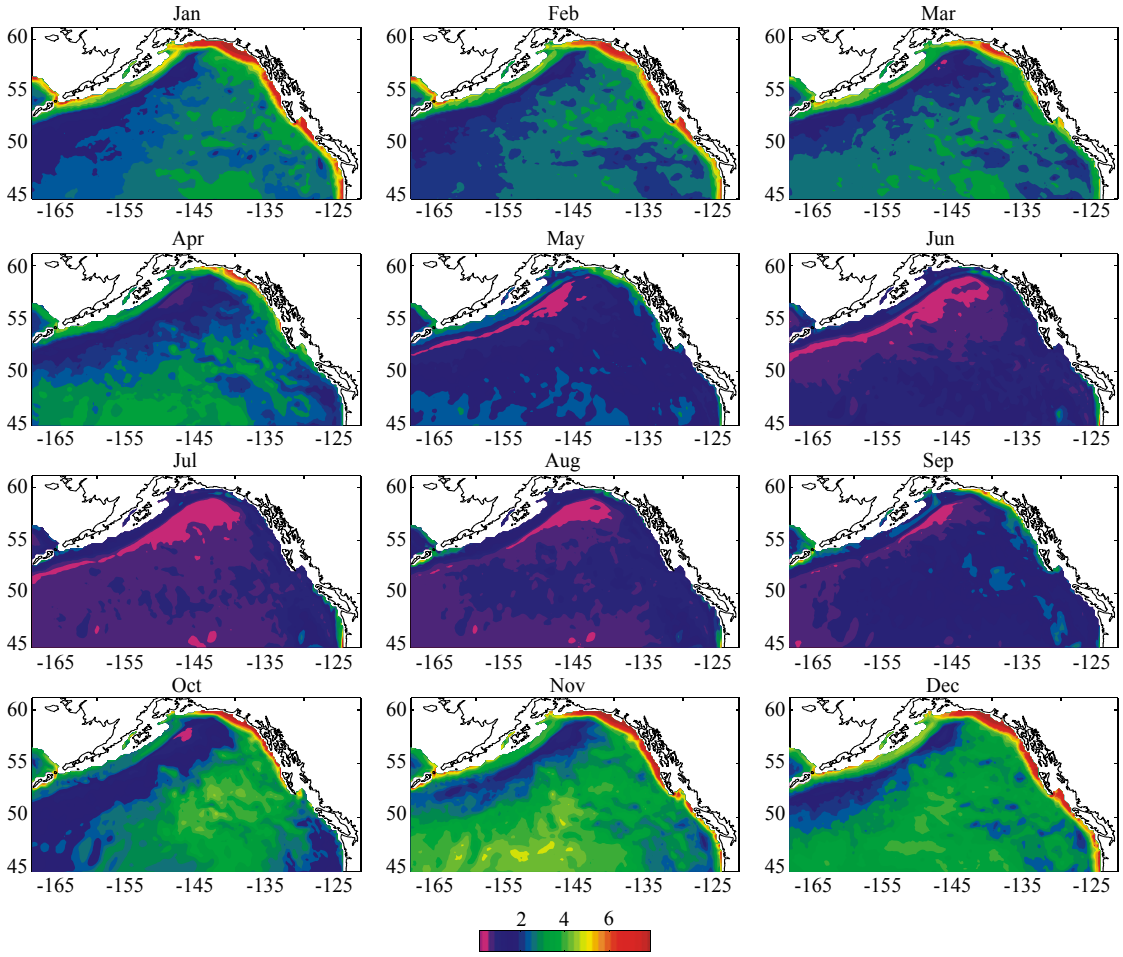

Figure 11: Seasonal Variability of the Eady Index, units in 10-6 s-1

coastal and topographic geometry. This geographical focusing combined with LaCasce and Pedlosky (2004) theory could explain why the amplitude of the eastern basin eddy field is proportional to the perturbation energy of the downwelling winds. Specifically during downwelling conditions in winter, the early response of the coastal ocean is linear with the onset of stronger poleward currents associated with the high coastal SSHa, and with the initial radiation of Rossby and topographically trapped waves. However because of the fast growth rate of the instability and the geographical focusing, most of the perturbation energy is locally trapped until converted into the eddy field. Although more

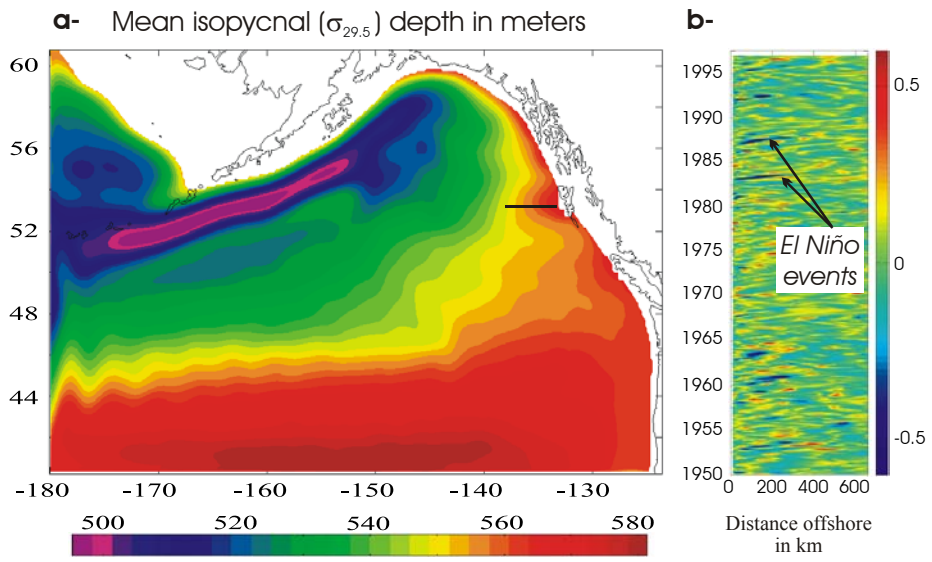

Figure 12: (b) shows Hovmuller diagram of the deseasonalized Ertel Potential Vorticity (s) along the black line represented in (a). (a) illustrates the depth of the 29.5 isopycnal in meters

detailed studies are needed, this energy trapping mechanism would explain the strong relationship between the perturbation amplitude of the winds and eddies.

These results also imply that the coherent-eddy like features that make it in the gyre interior are nonlinear and entrain coastal water masses. This is confirmed by inspecting the model Ertel potential vorticity (PV) field on isopycnal surfaces. A Hovmöller diagram on isopycnal 29.5 along a cross-shore transect in proximity of the region of Haïda eddies (Figure 12), shows strong entrainment and transport of low PV waters from the coast into the gyre interior. PV can be considered a passive tracer on isopycnal surfaces that do not exchange properties with the surface. In this case the low PV signature of the advected waters is associated with the southern origin of the entrained water masses at the coast, which are transported by the northward coastal currents. Some of the large ENSO events are reflected in the propagation of a strong PV minimum. The advection of water masses inferred by the PV analysis is consistent with

observational studies suggesting that eddies play a significant role in the cross-shore transport of iron-rich water masses (Johnston et al. 2005; Crawford et al. 2005).

4.2 INTRINSIC REGIME IN THE WESTERN BASIN

While the development of mesoscale eddies on the eastern GOA basin is modulated by changes in the wind stress, eddies along the Alaskan Stream (western basin) do not correlate with atmospheric forcing and their variability may be intrinsic (Okkonen et al. 2001). To separate the intrinsic and forced variability in the GOA we conduct an additional long-term (300 years) model run forced by climatological monthly mean surface fluxes (momentum, heat and freshwater; Experiment 2; Table 1). We refer to Experiment 2 as the "Unforced Run", in that there is no forcing function with periodicity longer than the seasonal cycle. In contrast, Experiment 1, which is forced by the time dependent NCEP winds and NOAA SST, is referred to as the "Forced Run". We then separate the SSH variance of the "Forced Run" and "Unforced Run" into "seasonal" (defined as all frequencies $\geq$ seasonal) and "interannual" (all frequencies lower than seasonal) (Figure 13a, b, d, e). First inspection of Figure 13 (a, b, c) shows that both runs exhibit similar seasonal variances with higher values along the coast where the seasonal winds drive the coastal current. A map of the difference in seasonal variances (Figure 13c) shows that the "Unforced Run" has slightly higher variance at the generation sites of Haïda and Sitka eddies. This is expected because the large interannual eddy events in

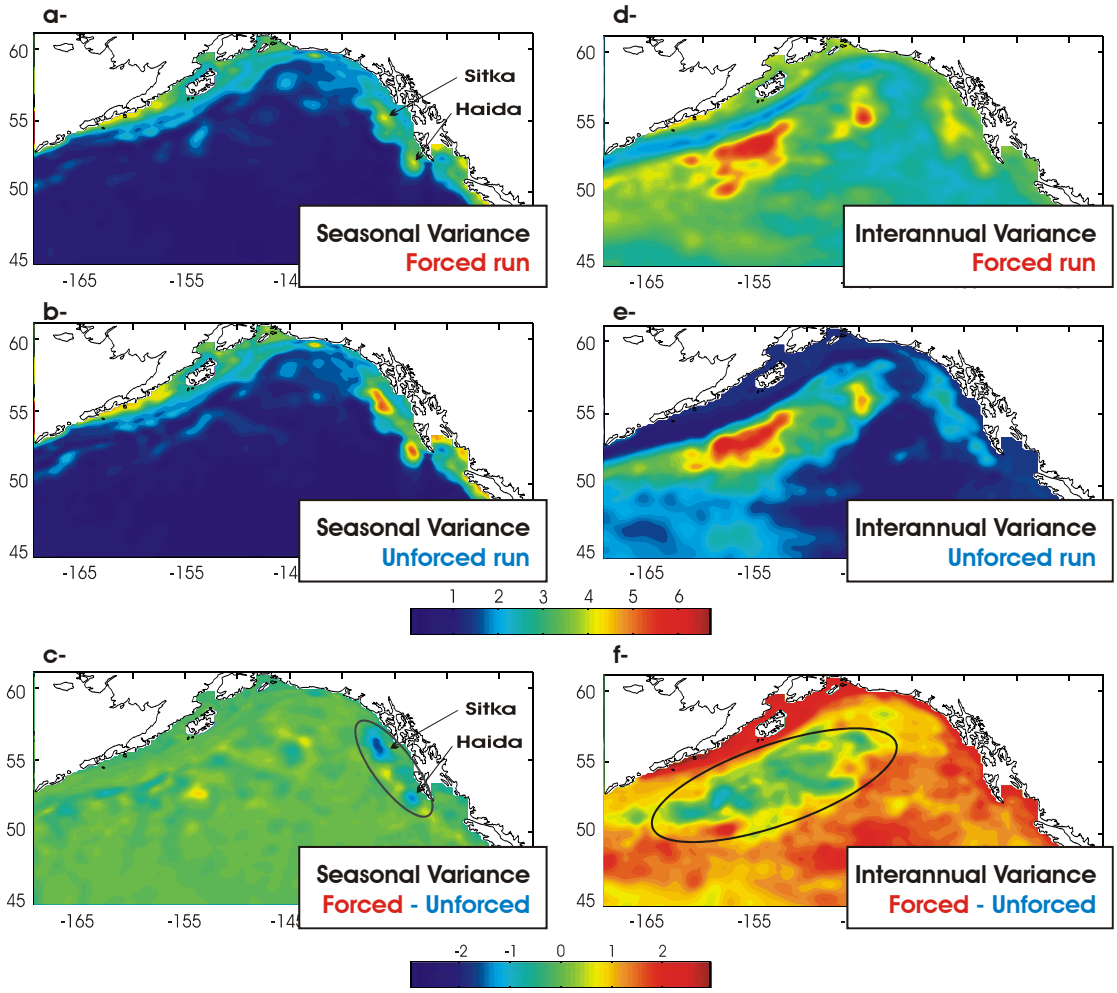

Figure 13: Model SSH standard deviations for the run forced by monthly NCEP wind stress (1st row) and for the run forced by climatology monthly wind stress (2nd row). The difference between the two runs is shown in the 3rd row. The first (second) column shows the seasonal (interannual) variance

these regions are phase locked with the seasonal cycle (see previous discussion of Figure 7), therefore some of the seasonal variance is shifted to the lower frequencies in the "Forced Run". If we now compare the maps for the "interannual" variance we find that the "Unforced Run" (Figure 13e) has strong variance in regions of high eddy activity in both the western and eastern basin. Since this model run has no forcing on periodicities higher than seasonal, regions of high variance must be associated with internal ocean (intrinsic) variability. To assess the degree of intrinsic variance we take the difference in variance between the "Forced" and "Unforced" (Figure 13f). Three important features can be isolated. First we observe that in the western basin (Figure 13f) there is no significant difference in interannual variance between the "Forced" and "Unforced" run. This confirms that most of the variance in the region of high eddy activity along the Alaskan Stream is intrinsic in nature. A second important feature in the difference map is in the shelf region along the western basin coastline. Here the "Unforced Run" has no variance when compared to the forced. This confirms that interannual changes in shelf circulation are mostly forced by the winds and it explains why the model "Forced Run" ensembles are so favorably correlated with in situ tide gauges (as shown before in the discussion of Figure 10). The third feature is in the eastern basin, where the "Forced Run' has higher variance along the eastern boundary. This result agrees with earlier results indicating that interannual changes in the winds force large anticyclones eddy such as Haïda and Sitka.

To further isolate the intrinsic and forced variability we compare timeseries from all "Forced" model ensembles in four selected regions of eddy activity, two in the western basin and two in the eastern basin (Figure 14 a, c, e and g). These timeseries

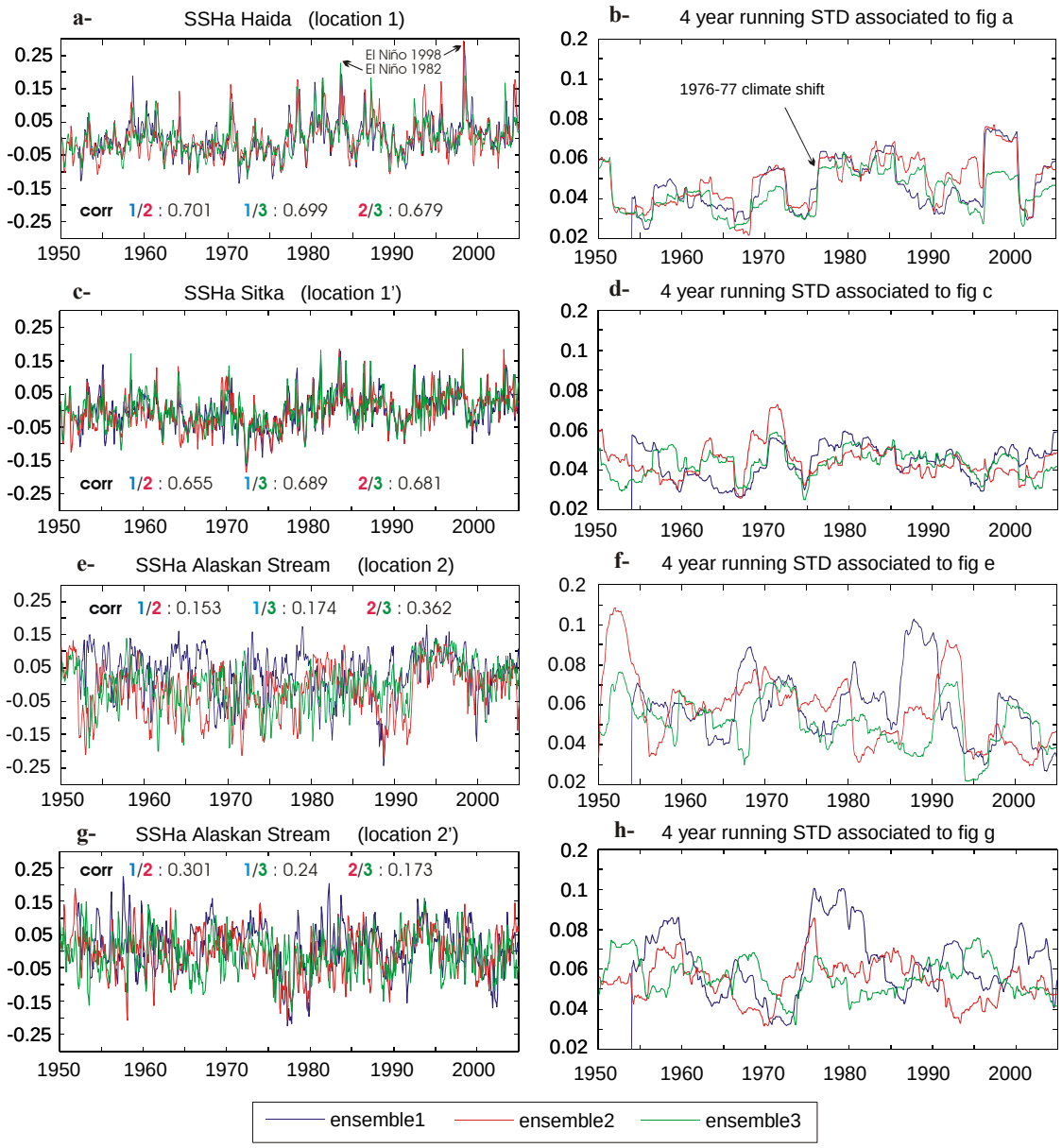

Figure 14: For the 3 ensembles (1,2,3), (a), (c), (e) and (g) show the SSHa respectively in the location 1, 1', 2 and 2' represented on Figure 2b. (b), (d), (f) and (h) show the 4 year running standard deviation associated to (a), (c), (e) and (g). (corr = correlation coefficient)

show that in the eastern basin (Figure 14a, c) the spread of the ensemble members is very low with shared variance above 42%. This confirms again the existence of a forced regime. In contrast in the western basin the ensembles members share little variance (Figure 14e, g) and are mostly uncorrelated with each other. Some low frequency variability after 1990 is shared by all the ensemble members in the western basin, with an indication of a negative trend, however the amount of explained variance by this component is small. Interestingly a comparison with satellite data (not shown) reveals a similar negative trend over the last 10 years, however we did not pursue this aspect further as the temporal data coverage is short.

Although eddy variability in the western basin is intrinsic, one may expect that changes in variance from year to year can be related to changes in the mean ocean conditions or forcing function. To explore this concept we compare the 4-year running standard deviation for all ensembles (Figure 14, right column). Inspection of the time series for the eastern basin shows a strong degree of correlation among all ensembles implying that interannual changes in eddy variance are also forced. In contrast in the western basin the spread among the ensemble members is high, although there are periods in the record when the ensembles are closer to each other. This reinforces the idea that changes in the forcing have a weak impact in modulating the eddy variance on interannual timescales.

We also investigate if ENSO teleconnected atmospheric forcing may play any role in changing the conditions for baroclinic instabilities, which is thought to play an important role in maintaining the western basin eddy field. We quantify the ENSO effect by correlating the instability growth rate (the Eady Index) with the NINO34 index

(Figure 15). The spatial pattern of the correlation shows that along the eastern boundary and northern Gulf of Alaska, an increase in the instability growth rate is positively correlated with positive ENSO phases. In contrast along the Alaskan stream in the region of high SSHa eddy variance, and in the gyre interior, we find a negative correlation indicating that during El Nino the growth rate is reduced. However the amount of negative correlation is insignificant, which confirms the intrinsic nature of eddy variability in the western basin.

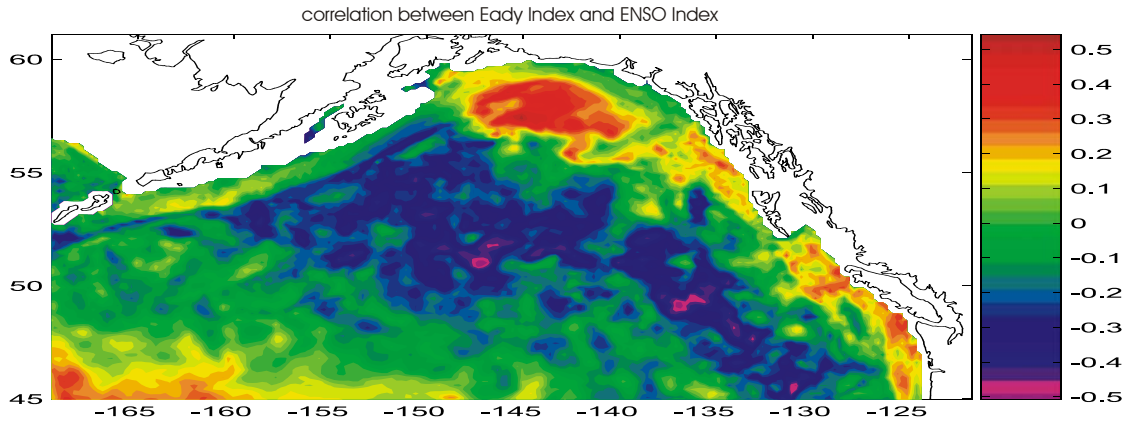

Figure 15: Map of the correlation between Eady index and ENSO index.

CHAPTER V

SUMMARY AND CONCLUSIONS

The adjustments of the Gulf of Alaska circulation to changes in large scale climate forcing has been investigated using three high resolution ensembles of a regional ocean model forced with the 1950-2004 NCEP winds and NOAA SST corrected heat fluxes. Consistent with previous descriptions of the circulation we find that the mean currents are mainly geostrophic (Figure 2a) and maintained by Ekman downwelling conditions in the eastern basin and upwelling along the Alaskan Stream (Figure 2b, c). On interannual and decadal timescale the mean circulation is strongly modulated by changes in the large scale climate forcing associate with PDO and ENSO (Figure 3). The leading mode of spatial and temporal variability of the mean currents in the three model ensembles is significantly correlated with the PDO (0.64) and shows strong peaks during El Niños (e.g. 1997-1998). Intensification of the gyre scale circulation is found after the 1976-1977 climate shift, as well as during 1955-1960, 1965-1970 and more gradually during 1993-1995. A detailed analysis of the model momentum and tracer budget reveals that when the GOA experiences stronger anomalous southeasterly winds (positive phase of the PDO after the 1976 shift and the 1997 ENSO) there is net Ekman convergence of surface mass (downwelling conditions) in the central and eastern coastal boundary (Figure 4b). This generates higher SSHa (Figure 4a) and lower isopycnals along the

coast. The resulting geostrophically adjusted currents (Figure 4a) intensify the gyre scale circulation. The opposite situation occurs during strong anomalous northwesterly winds (negative phase of the PDO).

Interannual changes in the surface winds are also reflected in modulation of the seasonal development of high amplitude anticyclonic eddies along the eastern basin, in particular at the location of the Haïda and Sitka eddies. The generation of the large interannual eddy events during winter-spring, is phase-locked with the seasonal cycle and is consistent with a quasi-linear Rossby wave response to stronger winter southwesterly winds typical of El Niño (Figure 7 and 8). The high correlation between the amplitude of the eastern basin eddy and the perturbation energy of the downwelling winds is explained by the combined effect of geographical focusing and instability of Rossby waves at higher latitudes (LaCasce and Pedlosky, 2004). Specifically during downwelling anomaly conditions, the early response of the coastal ocean is linear with the onset of stronger poleward currents associated with the high coastal SSHa, and with the initial radiation of Rossby and topographically trapped waves (Figure 7). However because of the fast growth rate of the instability (Eady index maps Figure 11) and the geographical focusing associated with the coastal geometry, most of the perturbation energy in the Rossby wave response is locally trapped until converted into the eddy field.

In the western basin, the high core of interannual eddy variability south of the Alaskan Stream (Figure 13d) is not correlated with large scale forcing and appears to be intrinsic. Indeed a comparison of the forced and internal interannual variability from the three forced ensembles and a multi-century-long integration forced only with the seasonal cycle of winds, heat and freshwater, shows that the intrinsic variance alone explains most

of the eddy variability (Figure 13f). The asymmetry between the eddy forced regime in the eastern basin and the intrinsic regime in the western basin is also confirmed by timeseries of the ensemble members SSHa. These show that along the eastern boundary the spread is very low with shared variance above 42% (forced regime). In contrast in the west, the ensembles members share little variance (Figure 14e, g) and are mostly uncorrelated (intrinsic regime), although some low frequency co-variability is evident after 1990. Coastal currents and SSHa on the shelf also respond to the wind forcing.

We also explored the possibility that ENSO atmospheric teleconnections may impact the degree of baroclinicity in the western basin. A spatial correlation analysis between the Eady index, which is a measure of the instability growth rate, and NINO34 index shows higher correlations along the eastern boundary and northern Gulf of Alaska. However no significant correlations are found in the center of high eddy activity of the western basin.

Although the eddy variability in the western basin is intrinsic, interannual changes in the shelf circulation are forced by the winds (Figure 13f). A comparison of SSHa between tidal gauges and the three model ensembles forced with the NCEP winds, reveals that the model is able to explain most of the variance with observational uncertainties. This finding suggest that most of the shelf variability on interannual scale does not strongly depend on equatorially trapped waves, but rather on downwelling (upwelling) conditions associated with the large scale wind stress patterns.

This study provides a dynamical framework to interpret and predict how the GOA circulation has and will respond to large scale climate forcing. The model analyses suggest that the adjustment to large scale climate forcing of the coastal and gyre-scale

mean circulations is predictable. On decadal and interannual timescale the most important aspect of the forcing is the overall strength of downwelling conditions along the coast, although the role of freshwater forcing has not been fully investigated. There is also strong indication of a basin-asymmetry in the response of the mesoscale eddy circulations. In particular eddy activity in the eastern basin is strongly correlated with changes in downwelling favorable winds, while in the western basin the variability is mainly intrinsic. The link between stronger eddy in the eastern basin and downwelling winds has important climate implications. It allows predicting changes in the cross-shore transport of important biogeochemical quantities such as iron, oxygen and chlorophyll-a, which in a global climate change scenario may contribute to feedbacks in the HNLC region of the GOA. Within the dynamical and modeling framework presented in this study, further analyses with higher resolution nested models will better resolve the mixing statistics associated with the eddy field in eastern and western basin. Model representations of the GOA circulation are in fact very sensitive to the coastal and topographic geometry. As such the model results presented so far should be interpreted more qualitatively rather than quantitatively.

REFERENCES

Brickley, P. J. and A. C. Thomas (2004). "Satellite-measured seasonal and inter-annual chlorophyll variability in the Northeast Pacific and Coastal Gulf of Alaska." Deep-Sea Research Part Ii-Topical Studies in Oceanography 51(1-3): 229-245.

Capotondi, A., M. A. Alexander, et al. (2005). "Low-frequency pycnocline variability in the northeast Pacific." Journal Of Physical Oceanography 35(8): 1403-1420.

Chelton, D. B., and M. G. Schlax, 1996: Global observations of oceanic Rossby waves. Science, vol. 272, pp. 234-238.

Crawford, W. R. (2002). "Physical characteristics of Haïda Eddies." Journal of Oceanography 58(5): 703-713.

Crawford, W. R. (2005). "Heat and fresh water transport by eddies into the Gulf of Alaska." Deep-Sea Research Part Ii-Topical Studies In Oceanography 52(7-8): 893-908.

Crawford, W. R., J. Y. Cherniawsky, et al. (2000). "Multi-year meanders and eddies in the Alaskan Stream as observed by TOPEX/Poseidon altimeter." Geophysical Research Letters 27(7): 1025-1028.

Crawford, W. R., P. Brickley, and A. Thomas, (2007). "Eddy Transport into a Cyclonic Gyre: An Example in the Gulf of Alaska." Progress in Oceanography, in press.

Cummins, P. F. and G. S. E. Lagerloef (2004). "Wind-driven interannual variability over the northeast Pacific Ocean." Deep-Sea Research Part I-Oceanographic Research Papers 51(12): 2105-2121.

Curchitser, E. N., D. B. Haidvogel, et al. (2005). "Multi-scale modeling of the North Pacific Ocean: Assessment and analysis of simulated basin-scale variability (1996-2003)." Journal Of Geophysical Research-Oceans 110(C11).

Di Lorenzo, E. (2003). "Seasonal dynamics of the surface circulation in the Southern California Current System." Deep-Sea Research Part Ii-Topical Studies in Oceanography 50(14-16): 2371-2388.

Di Lorenzo, E., M. G. G. Foreman, et al. (2005a). "Modelling the generation of Haïda Eddies." Deep-Sea Research Part Ii-Topical Studies In Oceanography 52(7-8): 853-873.

Di Lorenzo, E., A. J. Miller, N. Schneider, and J. C. McWilliams, (2005b). “The warming of the California Current: Dynamics and ecosystem implications”. Journal of Physical Oceanography, 35 (3), 336-362.

Gower, J. F. R. and S. Tabata (1993). "Measurement of eddy motion in the north-east Pacific using the Geosat altimeter." In Satellite Remote Sensing of the Oceanic Environment, ed. by I. S. F. Jones, Y. Sugimori and R. W. Stewart, Seibutsu Kenkyusha, Tokyo: 375–382.

Haidvogel, D. B., H. G. Arango, et al. (2000). "Model evaluation experiments in the North Atlantic Basin: simulations in nonlinear terrain-following coordinates." Dynamics Of Atmospheres And Oceans 32(3-4): 239-281.

Hoskins, B. J. and P. J. Valdes (1990). "On The Existence Of Storm-Tracks." Journal Of The Atmospheric Sciences 47(15): 1854-1864.

Hunt, G. L. and P. J. Stabeno (2005). "Oceanography and ecology of the Aleutian Archipelago: spatial and temporal variation." Fisheries Oceanography 14: 292-306.

Johnson, W. K., L. A. Miller, et al. (2005). "Iron transport by mesoscale Haïda eddies in the Gulf of Alaska." Deep-Sea Research Part Ii-Topical Studies In Oceanography 52(7-8): 933-953.

Kalnay, E., M. Kanamitsu, et al. (1996). "The NCEP/NCAR 40-year reanalysis project." Bulletin Of The American Meteorological Society 77(3): 437-471.

LaCasce, J. H. and J. Pedlosky (2004). "The instability of Rossby basin modes and the oceanic eddy field." Journal Of Physical Oceanography 34(9): 2027-2041.

Ladd, C., N. B. Kachel, et al. (2005). "Observations from a Yakutat eddy in the northern Gulf of Alaska." Journal of Geophysical Research-Oceans 110(C3).

Lagerloef, G. S. E. (1995). "Interdecadal Variations in the Alaska Gyre." Journal of Physical Oceanography 25(10): 2242-2258.

Levitus, S., R. Burgett, et al. (1994). World Ocean Atlas 1994. NOAA Atlas NESDIS 4, US Government Printing Office, Washington, DC, pp. 3-4.

Lindzen, R. S. and B. Farrell (1980). "A Simple Approximate Result For The Maximum Growth-Rate Of Baroclinic Instabilities." Journal Of The Atmospheric Sciences 37(7): 1648-1654.

Litzow, M. A., K. M. Bailey, et al. (2006). "Climate regime shifts and reorganization of fish communities: the essential fatty acid limitation hypothesis." Marine Ecology-Progress Series 315: 1-11.

Mantua, N. J., S. R. Hare, et al. (1997). "A Pacific interdecadal climate oscillation with impacts on salmon production." Bulletin Of The American Meteorological Society 78(6): 1069-1079.

Marchesiello, P., J. C. McWilliams, et al. (2003). "Equilibrium structure and dynamics of the California Current System." Journal of Physical Oceanography 33(4): 753-783.

Mellor, G. L., T. Ezer, et al. (1994). "The Pressure-Gradient Conundrum Of Sigma Coordinate Ocean Models." Journal Of Atmospheric And Oceanic Technology 11(4): 1126-1134.

Melsom, A., Meyers, S.D., Hurlburt, H.E., Metzger, E.J., O'Brien, J.J. (1999). "ENSO effects on Gulf of Alaska eddies." Earth Interactions 3 (1), (available at http://earthinteractions.org/).

Meyers, S. D. and S. Basu (1999). "Eddies in the eastern Gulf of Alaska from TOPEX POSEIDON altimetry." Journal Of Geophysical Research-Oceans 104(C6): 13333-13343.

Miller, A. J., D. Cayan, et al. (1994). "The 1976-77 climate shift of the Pacific ocean." Oceanography 7(1).

Miller, A. J., E. Di Lorenzo, et al. (2005). "Interdecadal changes in mesoscale eddy variance in the Gulf of Alaska circulation: Possible implications for the Steller sea lion decline." Atmosphere-Ocean 43(3): 231-240.

Murray, C. P., S. L. Morey, et al. (2001). "Interannual variability of upper ocean vorticity balances in the Gulf of Alaska." Journal Of Geophysical Research-Oceans 106(C3): 4479-4491.

Okkonen, S. R., G. A. Jacobs, et al. (2001). "Mesoscale variability in the boundary currents of the Alaska Gyre." Continental Shelf Research 21(11-12): 1219-1236.

Okkonen, S. R., T. J. Weingartner, et al. (2003). "Satellite and hydrographic observations of eddy-induced shelf-slope exchange in the northwestern Gulf of Alaska." Journal of Geophysical Research-Oceans 108(C2).

Rhines, P. B. (1986). "Vorticity Dynamics Of The Oceanic General-Circulation." Annual Review Of Fluid Mechanics 18: 433-497.

Sandwell, D. T. and W. H. F. Smith (1997). "Marine gravity anomaly from Geosat and ERS 1 satellite altimetry." Journal Of Geophysical Research-Solid Earth 102(B5): 10039-10054.

Shchepetkin, A. F. and J. C. McWilliams (2005). "The regional oceanic modeling system (ROMS): a split-explicit, free-surface, topography-following-coordinate oceanic model." Ocean Modelling 9(4): 347-404.

Smith, T. M. and R. W. Reynolds (2004). "Improved extended reconstruction of SST (1854-1997)." Journal Of Climate 17(12): 2466-2477.

Smith, W. H. F. and D. T. Sandwell (1994). "Bathymetric Prediction From Dense Satellite Altimetry And Sparse Shipboard Bathymetry." Journal Of Geophysical Research-Solid Earth 99(B11): 21803-21824.

Stabeno, P. J., N. A. Bond, et al. (2004). "Meteorology and oceanography of the Northern Gulf of Alaska." Continental Shelf Research 24(7-8): 859-897.

Stabeno, P. J. and A. J. Hermann (1996). "An eddy-resolving model of circulation on the western Gulf of Alaska shelf.2. Comparison of results to oceanographic observations." Journal of Geophysical Research-Oceans 101(C1): 1151-1161.

Strub, P. T. and C. James (2002). "Altimeter-derived surface circulation in the large-scale NE Pacific Gyres. Part 1. seasonal variability." Progress in Oceanography 53(2-4): 163-183.

Tabata, S. (1982). "The Anticyclonic, Baroclinic Eddy Off Sitka, Alaska, in the Northeast Pacific-Ocean." Journal of Physical Oceanography 12(11): 1260-1282.

Thomas, L. N. (2005). "Destruction of potential vorticity by winds." Journal Of Physical Oceanography 35(12): 2457-2466.

Thomson, R. E. and J. F. R. Gower (1998). "A basin-scale oceanic instability event in the Gulf of Alaska." Journal Of Geophysical Research-Oceans 103(C2): 3033-3040.

Whitney, F. and M. Robert (2002). "Structure of Haïda eddies and their transport of nutrient from coastal margins into the NE Pacific Ocean." Journal Of Oceanography 58(5): 715-723.